First Large Sample Study of Visible Light Photon Counters (VLPC's)

D. Adams, M. Adams, B. Baumbaugh, I. Bertram, A. Bross, D. Casey, S. Chang, M. Chung, C. Cooper, C. Cretsinger, R. Demina, G. Fanourakis, T. Ferbel, S. Grünendahl*, J. Hinson, B. Howell, H. Johari, J. S. Kang, C. L. Kim, S. K. Kim, D. Koltick, F. Lobkowicz, S. Margulies, J. Moromisato, M. Narain, C. H. Park, S. Reucroft, Y. M. Park, R. Ruchti, J. Solomon, E. VonGoeler, J. Warchol, M. Wayne, E. Won, Y. Yu

Fermi National Accelerator Laboratory, University of Illinois at Chicago, Korea University, Kyungsung University, Northeastern University, University of Notre Dame, Purdue University, Rice University, University of Rochester, Seoul National University

corrected version (VLPC structure)

Characterization of a large number of visible light photon counters (VLPC) is an integral part of the scintillating fiber system test for the D0 upgrade, currently underway at Fermilab. We report results from our investigation of 4200 channels of HISTE IV VLPC's, for use in a cosmic ray test. We have studied the dependence of critical device characteristics like quantum efficiency, gain, and noise as a function of operating temperature and VLPC bias voltage, and the variation of these characteristics over the large sample. We also discuss the general operation of the devices and the problems encountered during the characterization.

1. Introduction

In 1998, DØ will upgrade the central tracking region of the detector with an entirely new system consisting of a 2 Tesla superconducting solenoid, a 6000 channel preshower detector made of scintillator with wavelength shifting fiber read-out, an outer 80000 channel scintillating fiber tracker and an inner 837,000 channel silicon strip tracker[1]. The optical signal from the fibers will be detected by Visible Light Photon Counters(VLPC's). VLPC's are arsenic doped silicon diodes that operate near a temperature of 6.5 K with a bias of approximately 6.5 V[2]. High quantum efficiency, relatively high gain with low dispersion, combined with high signal forming speed and low noise, make these devices interesting for many high energy physics applications, in particular fiber tracking.

Since no experiment has ever used a fiber tracker read-out with many thousands of VLPC's, we decided to build a scaled-down version of the final fiber tracking system, triggering on cosmic rays. The Cosmic Ray Test Stand is a 3072 channel prototype of the final fiber tracker in the D0 upgrade. The primary purpose for this facility is to confirm that operation of large numbers of VLPC's is feasible and well understood. The detailed examination of the characteristics of the VLPC's is the subject of this report. In particular we focus on understanding the general operating parameters of the VLPC's, on determining the optimal operating points for the devices in the sample, and on issues like homogenity of the sample, yield, and a quantitative investigation of failure modes.

2. The VLPC

VLPC's are impurity band conduction silicon diodes, designed to convert single photons in to many thousands of electrons with high quantum efficiency. In contrast to standard avalanche photo diodes, only one of the two carrier types participates in carrier multiplication, which takes place across a band gap of only 50 meV, thus reducing gain dispersion considerably. The small gap is due to the formation of an impurity band 50 meV below the conduction band, created by

*Representing the DØ Collaboration.

a high donor concentration ($\approx 10^{17}/\mathrm{cm}^{-3}$) and low counterdoping ($\approx 10^{15}/\mathrm{cm}^{-3}$) in the p-layer of the diode.

A photon enters the VLPC through an antireflection coating and a transparent anode metalization, and creates an electron-hole pair across the standard valence-to-conduction band gap in the intrinsic (non-doped) zone. The hole drifts through the high field depletion region ('gain layer') and into the impurity band p zone ('drift layer'). Upon collision with a neutral donor, it frees an electron which starts the electron avalanche by impact ionization on neutral donor impurities. Due to space charge effects (created by the slowly drifting cloud of D^+'s) the avalanche process is self-limiting, and the gain saturates at a few 10^4. The precise value depends on the layer geometry and dopant concentrations.

A VLPC differs from a Solid State Photomultiplier (SSPM), its infrared-sensitive predecessor, only in so far as there is no need for an extended impurity band layer beyond the gain region. In the SSPM, infrared photons are converted in this layer. In the VLPC, only a small 'spacer region' of highly doped material is necessary to prevent break-through of the positive space charge to the buried cathode contact, which consists of the substrate silicon doped beyond the semiconductor-metal transition.

3. VLPC Mounting

The VLPC chips are produced by Rockwell [3] and are supplied as 1×8 pixel arrays with individual pixels of 1 mm diameter. The first step of the assembly process, done by an outside contractor[4], is to mount and wire-bond the arrays to an aluminum-nitride substrate[5]. The substrate provides the electrical contacts to the VLPC, via metalized castellations. The resulting combination of the substrate plus an 8 channel VLPC array is called a hybrid. Each hybrid is mounted in a molded plastic (Torlon) carrier at FNAL. Care must be taken to align the VLPC pixels (1 mm diameter on 1.05 mm centers) with holes (for later insertion of light-guide fibers) in the Torlon carrier. This is accomplished by a high-resolution video alignment system which provides mounting accuracies of 10 μm and thus assures that later the fibers are centered on the pixels to the required accuracy. It is in this form, as a hybrid mounted in a Torlon carrier, that the VLPC's are tested and characterized.

4. Test Stand

The fixture that eventually holds the VLPC's in line with optical fibers carrying the light signal from the tracker, and serves as enclosure for insertion into the cryostat, is called a cassette. There, the plastic carrier serves both the purpose of mounting the hybrid into the copper isotherm at the cold end of the cassette, and for aligning the optical fibers with the VLPC pixels, which are glued permanently into cylindrical slots in the Torlon carrier. For the characterization however, the VLPC's are temporarily mounted in a special test cassette (Figures 2 and 3). This test cassette does not require any soldered electrical connections or gluing of fibers. The test cassette holds 8 hybrids (= 64 VLPC pixels) at one time. During the characterization, we tested 7 new hybrids in each cool-down, using one slot to monitor run to run light level variation. The primary features of the test cassette are the following:

i) Light Distribution– Light from a red LED was used to pulse the VLPC's. A red LED was chosen because of its fast response to drive pulses. The VLPC's show relatively flat response in the visible spectrum, so the use of a red light rather than a green one should not compromise the measurements. The light from the LED is diffused by a scored piece of acrylic and brought to each VLPC by an individual optical fiber, whose diamond-polished end sits about 5 mm above the VLPC surface.

ii) Removable Torlon Carriers– The slots for the hybrids were designed for easy insertion and removal of the carriers. The bias supply and readout lines are connected to the substrate by single wire, gold plated springs, which contact gold-plated castellations on the hybrid. The spring alignment with the hybrid turned out to be non-trivial, due to minute variations in the VLPC chip position on its substrate (the alignment be-

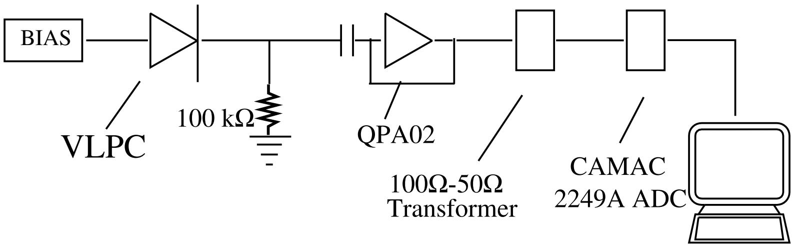

Figure 1. Signal flow diagram for the VLPC characterization test stand.

tween VLPC and Torlon carrier was guaranteed to $10\mu m$, but not the VLPC mounting on the substrate). Therefore the electrical contact was checked by a warm resistance measurement for each individual pixel, before the cassette was cooled down for VLPC characterization.

iii) IR tightening– Since the VLPC's are sensitive to IR radiation, care must be taken to shield the devices as much as possible from IR originating at the warm end of the cassette. In the test cassette, the optical fibers were fed through copper baffles, and layers of black felt were inserted between and around the optical fibers and electrical cables close to the hybrids, to block the IR light path from the warm end of the cassette. (In the final cassettes, the optical fibers, which themselves absorb IR light quite efficiently, terminate closer to the VLPC surface –about $50\mu m$ at low temperature–, thus making IR shielding somewhat easier.)

A VME-based low voltage supply designed at Fermilab supplied the bias voltage to the VLPC's. The signals were read-out through a QPA02 preamplifier, also designed at Fermilab. This transimpedance amplifier has a gain of approximately 2000 and a rise time of about τ_r=5 ns [7]. The preamp output signals are then transformed from double ended 100 Ω to single ended 50 Ω before going into CAMAC 2249A ADC's. We read the ADC's through a PC. The data was transferred to a VAX 4000-60 for analysis.

The VLPC's were cooled using liquid helium through a flow cryostat system[6]. The temperature was computer controlled to a tolerance of ∼0.1K.

5. Data Taking and Systematic Errors

We took data at 5 bias points (V=5.9 -7.1 V, ΔV=0.3 V) and 4 temperature points (T=5.5 - 7.0 K, ΔT=0.5 K). For each pixel, two spectra were taken at each point. One was taken with no light to obtain the pedestal value, and one with a light pulse corresponding to an average of ∼2 photoelectrons at 6.5 K and 6.5 V. Each spectrum contained 20000 events; the integration time in the ADC for each event was 90 ns.

Run to run errors due to the mechanical (rather than soldered) connections, handling of the light guide, and general changes in the cassette due to thermal cycling were kept at ∼2%. Run to run light levels were monitored by keeping a single chip in the same slot throughout the calibration. The channel to channel gain variation of the preamp was measured to be ∼3%. Each VLPC channel has a 100 kΩ current limiting resistor. Since each VLPC, under normal operating conditions, draws a significant amount of current (∼1 μAmp/channel at 6.5 V and 6.5 K), there is a VLPC bias offset of ∼ 0.1V depending upon the current. The cumulative contribution of these effects on the gain and the observed number of photoelectrons results in an ∼5% systematic uncertainty.

There was also a channel to channel light level variation in the cassette. We measured the variation by cycling a single hybrid (the same hybrid that was used throughout the characterization to monitor the run to run light levels) through each of the positions in the cassette and measuring the number of photoelectrons. Since the

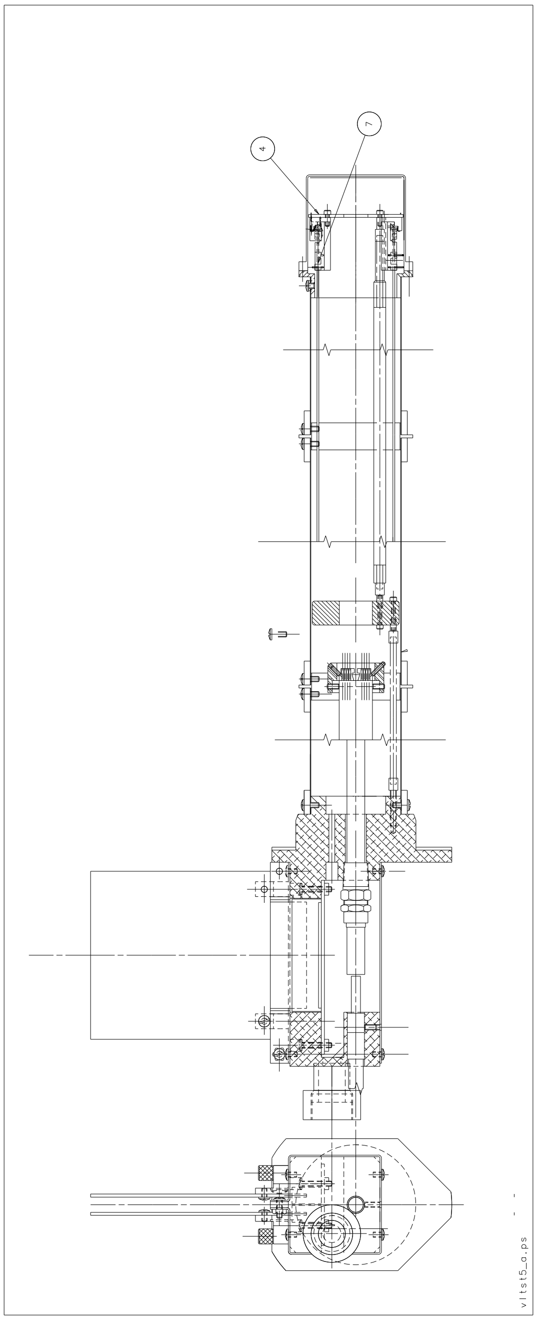

Figure 2. VLPC test cassette: side and top view

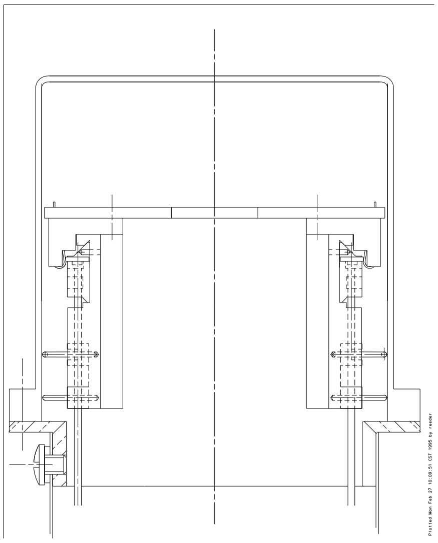

Figure 3. Cold end detail of the VLPC test cassette, showing hybrid holder with optical fibers and VLPC contact springs

run to run variations were small, we assumed that all of the variations observed were due to light level changes from channel to channel in the cassette and from intrinsic QE variations across the calibration chip. In extracting the data on the relative quantum efficiency, we further assumed that the variation observed was due primarily to light level variation in the system and not due to QE variations across the hybrid. To verify this assumption, we iterated three hybrids (including the previously mentioned 'calibration chip') through each of the slots in the cassette and found that the observed light levels were the same within a given slot to better than 5%.[2] The final light level correction factor was determined by referencing the light level in all 64 channels (determined from the iteration of a single hybrid through the 8 slots) to the first channel. The total systematic error on the relative quantum efficiency is then ~7%.

6. Raw Data

Figures 4,5 and 6 show the three basic types of

[2] The absence of QE variations across a hybrid is supported by additional measurements performed in the meantime by Rockwell, which found no systematic variation in a pixel scan across a wafer.

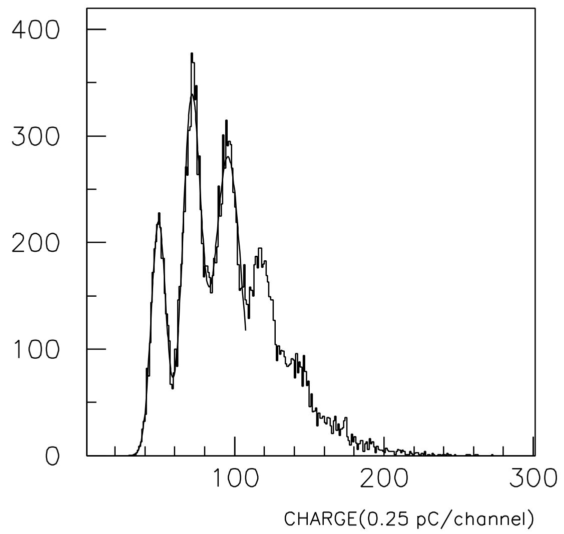

Figure 4. A typical spectrum from a good VLPC pixel at T=6.5 K and U=6.5 V.

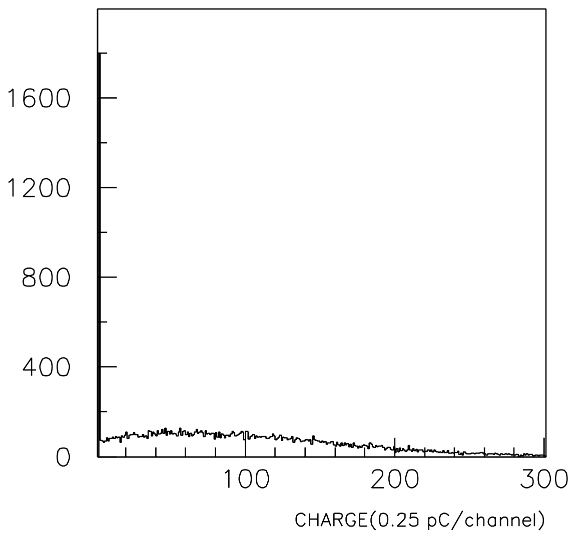

Figure 5. Spectrum showing a failed ('latched') VLPC pixel; T=6.5 K and U=6.5 V.

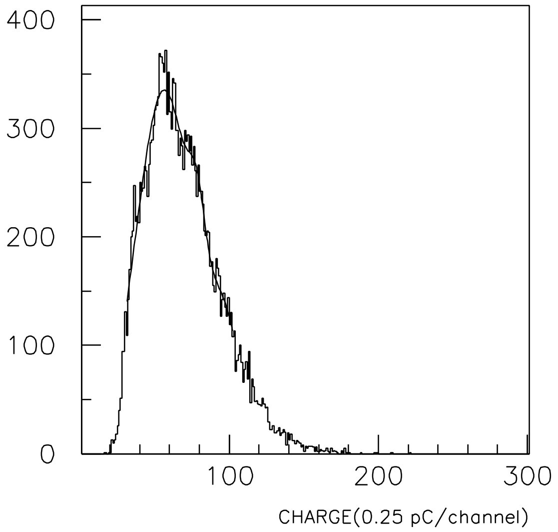

Figure 6. Spectrum showing IR smearing from a VLPC pixel at T=6.5 K and U=6.5 V.

spectra that were observed. Figure 4 shows a typical good spectrum. There is clean separation between the pedestal, first and second photoelectron peaks and often one sees structure for the third, fourth, or even fifth photoelectron peak. (Note the the light level was set to peak at ~2 photoelectrons at this temperature and bias.) Figure 5 shows a typical bad channel. Such pixels were observed to have very noisy oscilloscope signals and drew ten times more current than pixels that operated properly. Interestingly, some of these pixels seemed to radiate light to adjacent pixels on the same chip, causing the photopeaks to smear. This high-current effect has also been observed in SSPM's, of which we characterized fifty in the same apparatus, and there it has been shown that the effect was due to latch-up of the devices. In the SSPM, one could restore proper operation by lowering the bias to 1 or 2 volts. Further testing of the VLPC's revealed that they did not exhibit this toggling effect, but were, in fact, locked into the high-curent state and could not be restored to normal operation. Diasabling these latched pixels, by disconnecting their bias line, restores proper operation of their neighbouring channels. Figure 6 shows a spectrum marred by an IR light leak. These signals show the proper number of photoelectrons, but there is little to no separation between the individual photoelectron peaks. Electrically noisy but non-latched pixels show a similar type of spectrum, as do neighbours of photon-radiating latched pixels. One should note that for applications like the D0 fiber tracker, where each signal typically contains ≈ 10 photoelectrons, single photoelectron separation is not important. Thus, such pixels with intrinsically bad single photon resolution are useable as long as their noise rate is not excessively high.

7. Results

Figure 7 shows the distributions for gain, raw and corrected (for light level nonuniformity in the test cassette) relative quantum efficiency, and dark count rate for the whole sample at the nominal operating point. The accumulation of entries at half the nominal gain is due to defective preamplifier channels.

Figure 8 shows the dependance of the observed means and root mean square widths of these distributions on temperature and bias. One sees the strong dependance of noise and gain on bias voltage, as the latter approaches the breakdown voltage, whereas the quantum efficiency approaches a plateau. As shown in [8], the optimum balance in this tradeoff between QE and dark count rate depends on the light levels to be detected in the particular application.

7.1. Dark Current and Noise

The dark count rate is measured by integrating the pedestal spectrum above a given threshold. The threshold (in photoelectrons) is computed using the gain and pedestal values as determined from the light pulser spectra. The noise rates shown in figures 8 and 7 are the count rates for a threshold of 0.5 photoelectrons. Typical values at standard operating conditions are around 200 kHz, a factor of 20-30 higher than achieved with both earlier SSPM and later VLPC generations; the excessive noise, which nevertheless does not compromise the use of these devices in our tracking application [8], is attributed to an antimony contamination in the boundary between blocking (intrinsic) and gain layer.

7.2. Gain

The gain is defined as the difference between the first and second photoelectron peak positions. At our nominal operating point of 6.5 V and 6.5 K, the gain is 12,400, with an rms of 15%. The rms of the normalised gain distribution varies from 9% at T=6.0 K, U=5.9 V, to 24% at T=7.0 K, U=7.1 V.

7.3. Quantum Efficiency

The relative QE is obtained by comparing the average number of photoelectrons observed from pixel to pixel and normalizing the distribution to an average QE of 60% at 6.5 K and 6.5 V.[3] The rms of the normalised quantum efficiency distribution is 16%±2% for most values of temperature and bias.

7.4. Yield

We define as useable a chip which has zero dead or latched pixels. 520 hybrids have been characterized in total. Of those characterized, 320 were considered good at the test stand by looking at spectra from the T=6.5 K and V=6.5 V point, 120 appeared to have at least 1 bad (latched or dead) pixel, and 80 were considered marginal, due to one or more noisy but non-latched pixel, and were retested. Of the marginal chips re-tested, 34 were recovered as good chips. Due to an uncertainty concerning the reliability of some of the spring contacts (and some questions concerning the distinction between noisy and latched channels), in a second round of testing we recharacterized 111 of the 120 initially discarded chips, and found 47 to fulfill our acceptance criteria. This brings the total yield to 401 of 520 arrays. The recovery can be attributed to better contact with the read-out springs in the cassette.

[3] The 60% average is taken from QE measurements at Rockwell, referencing HISTE IV VLPC's to previously calibrated SSPM's. The absolute calibration of our test stand using photo diodes is still under way.

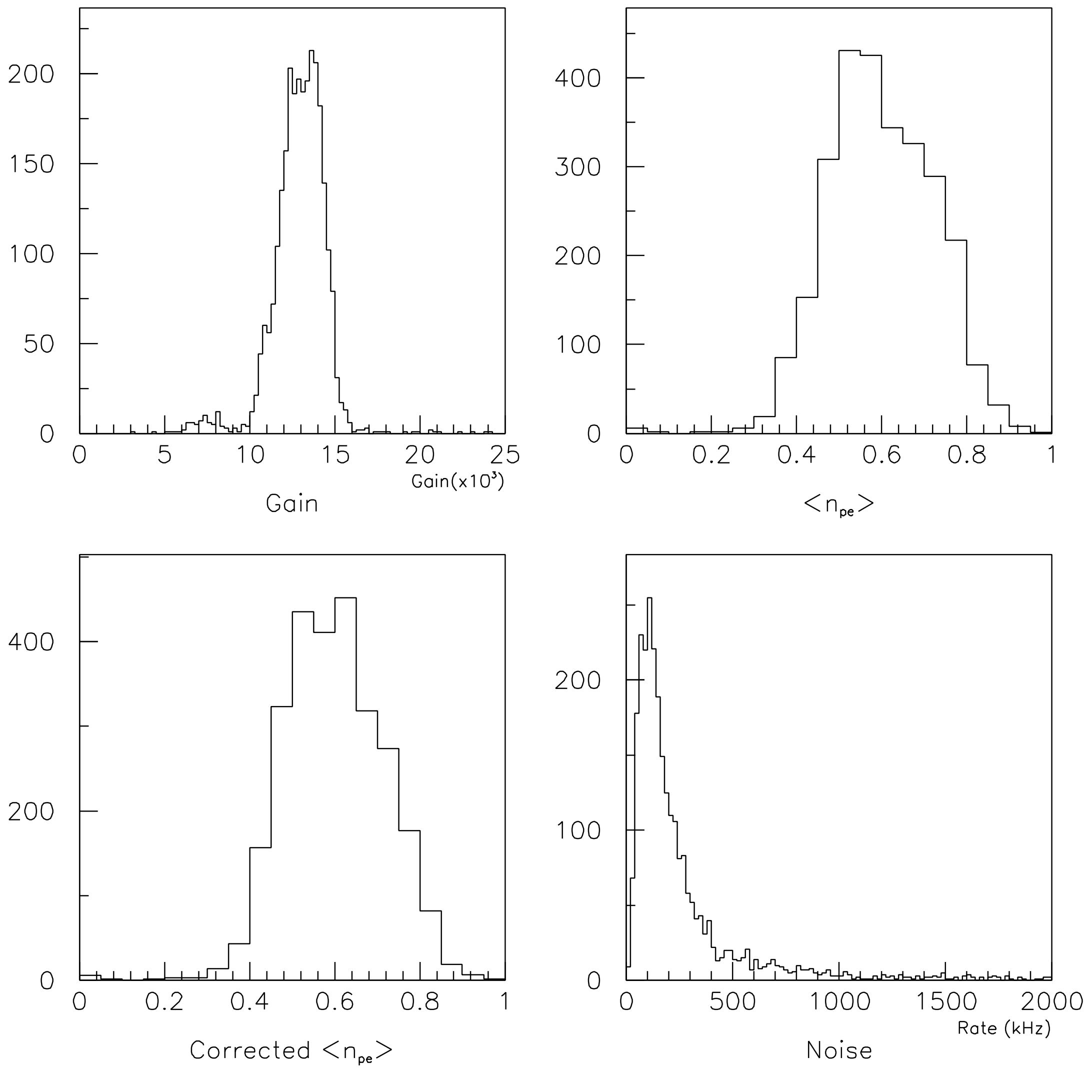

Figure 7. Gain, raw and light-level corrected QE, and dark count rate for a 0.5 PE threshold, for all characterized channels at T=6.5 K and U=6.5 V

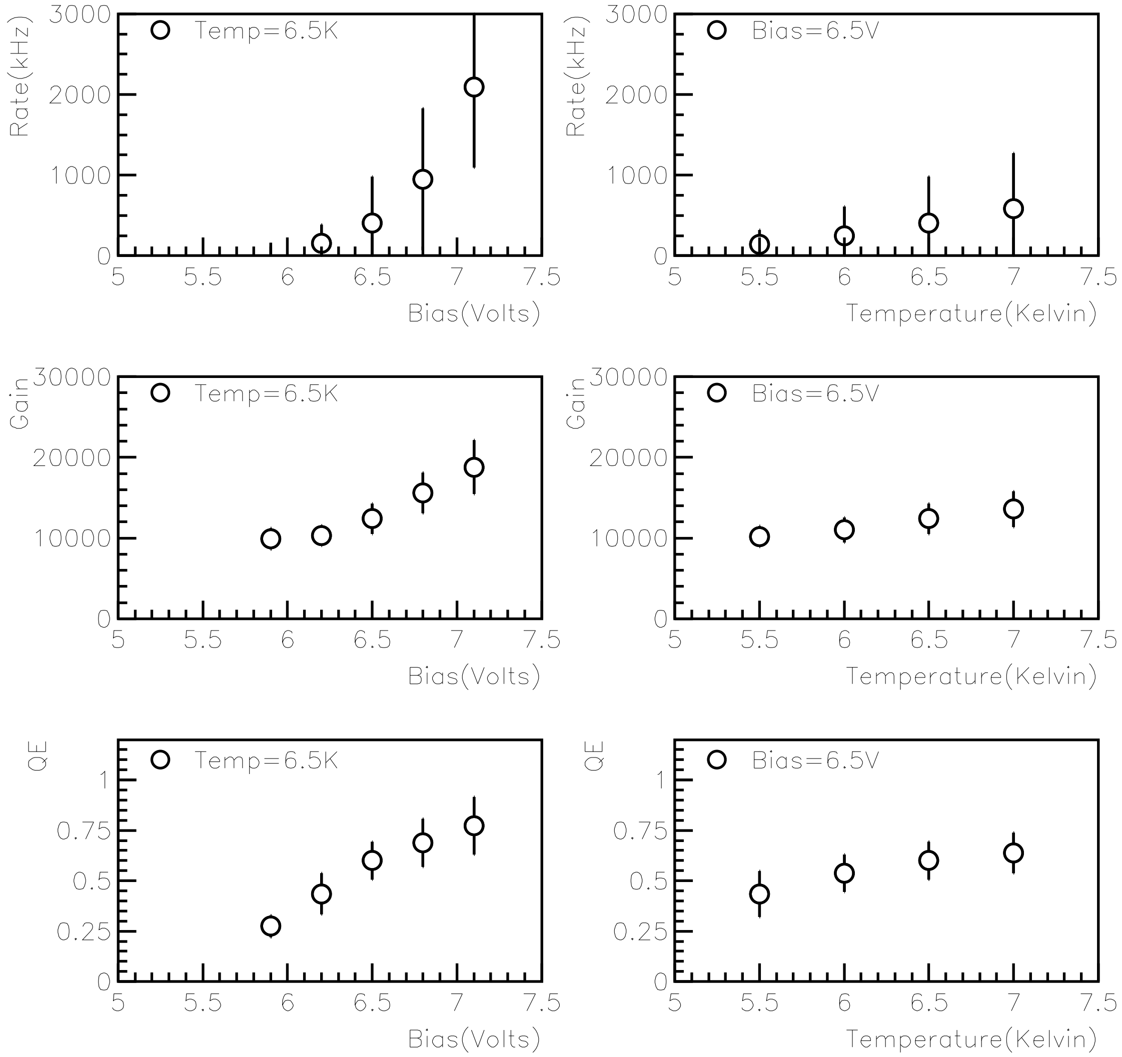

Figure 8. Sample mean and rms for dark current, gain, and QE as a function of VLPC bias at T=6.5 K, and as a function of operating temperature at U=6.5 V.

7.5. Conclusion

VLPC's exhibit superb characteristics as fast photon detectors for use in a low light level application. The sample of 4200 channels of VLPC's shows a high enough yield, and the working devices are homogenous enough in their operating parameters to make the use of VLPC's in large numbers feasible. Furthermore, the relatively high yield makes it attractive to test the devices after dicing and wirebonding, a strategy which we plan to adopt for the 80,000 DØ fiber tracker. Further tests, performed at Rockwell on the next generation of VLPC's, HISTE V, show that devices manufactured from substrate grown in a production (as opposed to experimental) facility, exhibit considerably narrower distributions of QE and gain, and a much lower dark count rate. We plan to characterize a sample of about 2000 channels of these devices in the near future.

8. Acknowledgements

This research is being performed with the generous support of the Department of Energy.

REFERENCES

1. E823 *(DØ Upgrade):DØ$_\beta$*, DØ Note 1733 (1993); A. Bross et al., Fermilab 1995, these proceedings.
2. M. D. Petroff, M. G. Stapelbroek, and W. A. Kleinhans, *Appl. Phys. Lett.* **51**, 406 (1987).
3. Rockwell International, Anaheim, CA.
4. Promex Microelectronics, Santa Clara, CA.
5. Carborundum Microelectronics, Phoenix, Arizona.
6. Oxford Continuous Flow Cryostat CF1200, Oxford Instruments Limited, Eynsham, England.
7. T.Zimmerman, *IEEE Trans. on Nucl. Sci.* **37** (1990) 439.
8. Performance of a 3000 Channel SciFi Tracker with VLPC Readout, Y.M. Park et al., Fermilab 1994, these proceedings.